catalysts

MDPI

Review

Recent Progress on MOF-Derived Nanomaterials as Advanced Electrocatalysts in Fuel Cells

Zhongxin Song, Niancai Cheng, Andrew Lushington and Xueliang Sun *

Department of Mechanical and Materials Engineering, The University of Western Ontario, London, ON N6A 5B9, Canada; zsong52@uwo.ca (Z.S.); ncheng26@uwo.ca (N.C.); andrew.lushington@gmail.com (A.L.)
* Correspondence: xsun@eng.uwo.ca; Tel.: +1-519-661-2111 (ext. 87759)

Academic Editors: Frédéric Jaouen and Keith Hohn
Received: 19 June 2016; Accepted: 22 July 2016; Published: 2 August 2016

Abstract: Developing a low cost, highly active and durable cathode material is a high-priority research direction toward the commercialization of low-temperature fuel cells. However, the high cost and low stability of useable materials remain a considerable challenge for the widespread adoption of fuel cell energy conversion devices. The electrochemical performance of fuel cells is still largely hindered by the high loading of noble metal catalyst (Pt/Pt alloy) at the cathode, which is necessary to facilitate the inherently sluggish oxygen reduction reaction (ORR). Under these circumstances, the exploration of alternatives to replace expensive Pt-alloy for constructing highly efficient non-noble metal catalysts has been studied intensively and received great interest. Metal–organic frameworks (MOFs) a novel type of porous crystalline materials, have revealed potential application in the field of clean energy and demonstrated a number of advantages owing to their accessible high surface area, permanent porosity, and abundant metal/organic species. Recently, newly emerging MOFs materials have been used as templates and/or precursors to fabricate porous carbon and related functional nanomaterials, which exhibit excellent catalytic activities toward ORR or oxygen evolution reaction (OER). In this review, recent advances in the use of MOF-derived functional nanomaterials as efficient electrocatalysts in fuel cells are summarized. Particularly, we focus on the rational design and synthesis of highly active and stable porous carbon-based electrocatalysts with various nanostructures by using the advantages of MOFs precursors. Finally, further understanding and development, future trends, and prospects of advanced MOF-derived nanomaterials for more promising applications of clean energy are presented.

Keywords: MOF-derived nanomaterials; fuel cells; electrocatalyst; oxygen reduction reaction

1. Introduction

1.1. Introduction and Challenges Facing Fuel Cell Devices

Fuels cells have the advantage of providing energy that is highly efficient with negligible environmental pollution and can be operated using virtually unlimited sources as reactants. These advantages have allowed fuel cells to develop into widespread commercial use in the fields of transportation, and stationary and portable electronics, and thus will help aid in addressing the global challenge of energy demand [1]. Among existing fuel cell technologies, the polymer electrolyte membrane fuel cell (PEMFC) merits low working temperature, high power density, and quick start-up, and has been actively developed to power future electrical vehicles, portable electronics and other energy-consuming devices [2–6]. Due to the recent progress in anion-exchange membranes capable of conducting hydroxide ions (OH^-), the alkaline fuel cells technology has been revitalized. As shown in Figure 1, each fuel cell consists of an anode, a cathode and electrolyte. In an alkaline fuel cell, oxygen as the reactant can be reduced into OH^- with the overall reaction of $O_2 + 2H_2O + 4e^- \rightarrow 4OH^-$ at

cathode side. The produced OH^- anions reach to the anode through the anion-exchange membrane electrolyte. At the anode side, hydrogen (H_2) as the fuel can react with the OH^- and produce H_2O and electrons ($2H_2 + 4OH^- \rightarrow 4H_2O + 4e^-$). The electrons are transferred to the cathode through an external circuit, while hydroxide ions reach the cathode through the electrolyte membrane. Both the anode and cathode electrodes consist of highly dispersed Pt-based catalysts loading on carbon support to promote the hydrogen oxidation reaction (HOR) and oxygen reduction reaction (ORR). The reaction rate of the HOR on Pt is sufficiently fast, therefore the required amount of Pt loading at the anode can be less than 0.05 mg·cm^{-2}. However, at the cathode, the sluggish reaction kinetics of the ORR requires a much higher Pt loading (~0.4 mg·cm^{-2}) to achieve appropriate fuel cell performance [7]. Pt-based precious metal catalysts still suffer from several critical problems, such as high cost, low abundance, poor stability, crossover effect, and CO poisoning [8,9]. These bottlenecks hamper the widespread commercialization of fuel cells. Therefore, reducing Pt loading, or even completely replacing it with a low-cost earth-abundant catalyst, without compromising performance, is a major challenge facing the application of this promising technology.

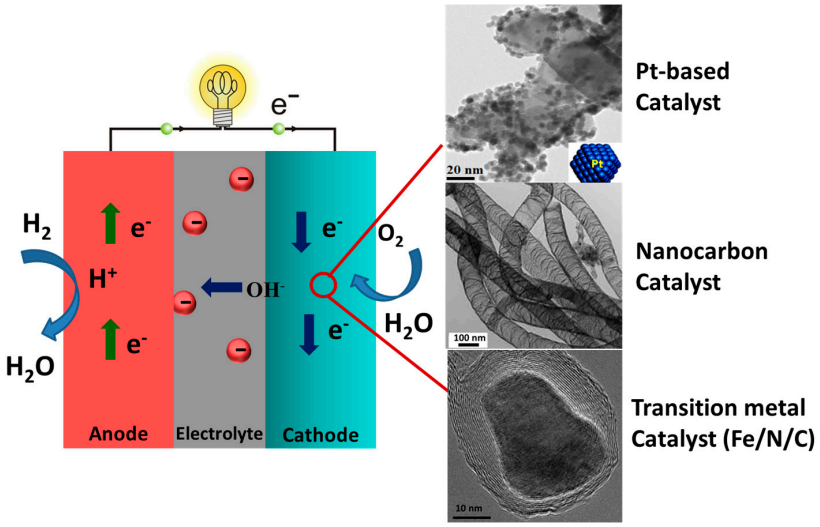

Figure 1. Illustration of typical pathways of oxygen reduction reaction in an alkaline fuel cell and three categories of the cathode catalysts used for oxygen reduction reaction (ORR).

Great efforts have been devoted to develop highly efficient, economical, and stable catalysts for ORR, including advanced Pt alloys, core-shell structures, heteroatom-doped-carbon, and transition metal/metal oxide-carbon composite catalysts (as shown in Figure 1) [10–15]. Among the non-noble metal catalysts, transition metal/metal oxide-carbon (e.g., Co/Co_3O_4-C, Co-Nx-C, Fe-Nx-C) [16–18] and heteroatom-doped-carbon materials (e.g., N-C, NS-C, NP-C) [19–24], have been a major focus of research due to their excellent electrocatalytic activity, high stability, and low cost. Particularly, the non-noble metal catalysts fabricated from MOFs precursors have been explored and demonstrate a number of advantages owing to their high specific surface area, porous structure, and abundantly high distribution of active sites. Furthermore, the novel method of fabricating transition metal/metal oxide-carbon electrocatalysts from the MOFs precursors, not only offers a new approach to further enhancing the catalytic activity, but also helps in overcoming the intrinsic activity and conductivity limitations of the existing transition metal/metal oxide nanoparticles.

1.2. A Possible Solution with the Use of MOF-Derived Nanomaterials

MOFs have emerged as an extensive class of crystalline materials with ultrahigh porosity and enormous internal surface area. These properties, together with the extraordinary degree of variety in organic and inorganic components, make MOFs materials particularly interesting for

application in fields such as catalysis, strategic gas capture and storage, and drug delivery [25,26]. The heterogeneous catalysis is one of the earliest demonstrated applications of crystalline MOFs materials [27]. A defining characteristic of MOFs is their porosity, yielding a relatively large internal surface area, thereby facilitating outstanding catalytic activity. Although the crystalline MOFs share efficient catalysis features, they still suffer from difficulties including poor conductivity and facile collapse during solvent extraction. To overcome these obstacles, MOFs can be used as a template and/or precursor to synthesize MOF-related nanomaterials. By delicate design of MOFs precursors, together with careful post-treatment, the advantages and catalytic activity of MOFs materials can be fully inherited by the MOF-derived nanomaterials. For example, MOF-derived heteroatom-doped nanocarbon [28–31], transition metal/metal oxide-carbon hybrids and composites (as shown in Figure 2) [26,32–36], with high surface area and porosity, have been reported to exhibit excellent catalytic activity and stability, while also displaying outstanding bifunctional activity toward ORR and oxygen evolution reaction (OER). It should be noted that MOFs precursors employed in developing heteroatom-doped nanocarbon can be conveniently tailored by coupling them with a second heteroatom-containing precursor. This duality allows for control over both chemical composition and porous structure of the final carbon product [37,38]. This review aims to summarize the recent progress toward the fabrication of MOF-derived nanomaterials as electrocatalysts for application in fuel cells. Importantly, we focus on the rational design and synthesis of highly active and stable porous carbon-based electrocatalsyts by taking advantage of MOFs precursors within the context of electrochemcial performance toward ORR, OER and HER.

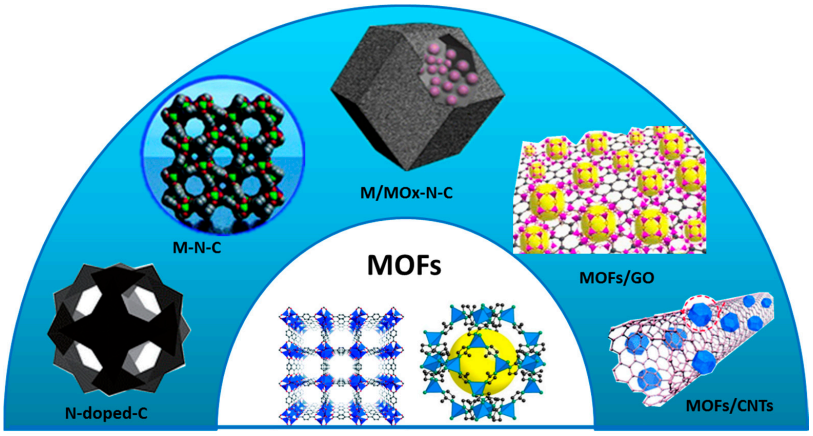

Figure 2. MOFs used as templates and/or precursors for fabricating the nanocarbon and related functional nanomaterials.

2. MOF-Derived Heteroatom-Doped Nanocarbon Electrocatalysts

The large content of carbon-based organic linkers in MOFs crystals aids in facilitating the fabrication of nanocarbon materials. In 2008, Xu's group demonstrated, for the first time, the application of MOFs as a template to synthesize nanocarbon materials [39]. Nanocarbon and related functional nanomaterials, obtained from MOFs, show attractive physical and chemical features, resulting in an increased amount of attention being fostered by fields associated with energy-related applications. Thus far, the functional porous heteroatom-doped nanocarbon materials have been considered as promising metal-free electrocatalsyts in fuel cells because of their unique physical and chemical characteristics, pronounced electrocatalytic activity, long-term stability, and relatively low costs [40–42]. Among them, single-doped nanocarbon (e.g., N-C) [37], multi-doped nanocarbon (e.g., NS-C, NPS-C) [43–46], as well as nanocarbon composites (e.g., nanocarbon/CNTs, nanocarbon/graphene) [28–31], have been researched as effective electrocatalysts in fuel cells.

2.1. N-Doped Nanocarbon Electrocatalysts

It was widely accepted that the incorporation of nitrogen atoms into the carbon lattice can significantly enhance the surface polarity and electron-donor tendency of the carbon matrix, resulting in advanced electrocatalytic performance towards ORR and/or OER [47–49]. Recently, zeolitic imidazolate frameworks (ZIFs) have been utilized as a template and precursor to create N-doped nanocarbon, due to their highly ordered nanoporous structure and imidazole-based organic linkers, resulting in an abundance of nitrogen incorporation. More importantly, during the high temperature carbonization process, the removal of corresponding metal species plays a significant role in facilitating the formation of highly porous structure. Recently, Hong and co-workers [37] reported the fabrication of in situ nitrogen-doped graphitic porous carbons (NGPCs) from pyrolysis of template ZIF-8. This method allows for the simultaneous incorporation of both carbon and nitrogen sources during the carbonization process. SEM and TEM images revealed that the NGPCs products inherit the original nanopolyhedron morphology of the parent ZIF-8. Meanwhile, the outstanding merits of rich nitrogen atoms, hierarchical porosity, as well as excellent conducting networks, have been endowed into the NGPCs. To illustrate the correlations between the mesoscopic structures and the electrochemical activity, a sample of NGPC-Tc-t was fabricated by carbonization of ZIF-8 precursor at different temperature T_c (T_c = 700, 800, 900, 1000 °C) and for various carbonization time (t = 1, 5, 10 h). The optimized NGPC-1000-10 nanoparticles (carbonized at 1000 °C for 10 h) demonstrated outstanding electrocatalytic performance toward the ORR, as reflected by its high current density of 4.3 mA·cm^{-2} at −0.6 V and a significant positively shifted onset-potential of −0.02 V (vs. Ag/AgCl) in 0.1 M KOH solution, both of which are close to the corresponding values of benchmark Pt/C catalyst (as shown in Figure 3). Therefore, it was noted that MOFs can be used as an ideal precursor to yield metal-free N-doped nanocarbon elelctrocatalysts for ORR. Furthermore, the authors revealed that the outstanding electrocatalytic activity of this true metal-free catalyst is attributed to the synergetic contributions of abundant graphitic-N active sites.

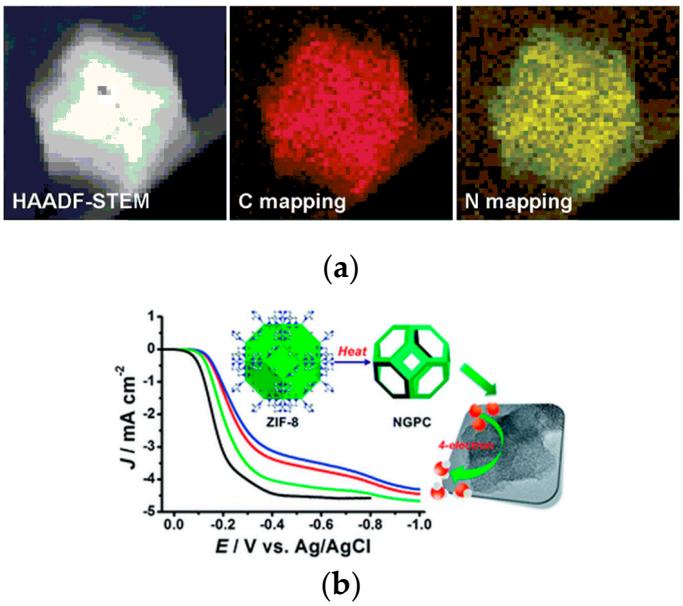

Figure 3. (**a**) HAADF-STEM images of a single NGPC polyhedron and the corresponding C-, and N-elemental mappings; (**b**) Linear sweep voltammetry (LSV) curves of Pt/C (**black**) and NGPCs obtained at 1000 °C with a carbonization time of 1 h (**red**), 5 h (**blue**), and 10 h (**green**) in O_2-saturated 0.1 M KOH at 1600 rpm with a scan rate of 5 mV·s^{-1} [37]. Copyright 2014, Royal Society of Chemistry.

Another method to fabricate N-doped nanocarbon materials is through the use of MOFs as a sacrificial template/precursor with incorporation of a second precursor to achieve in situ N-doped porous carbon with large surface area and narrow pore size distribution. Some organic compounds such as furfuryl alcohol (FA), glucose and melamine are employed for this purpose [39,50,51]. Briefly, the organic compound, as a second carbon and nitrogen precursor, is first infiltrated into the pores of the MOFs template, followed by a carbonization process at a high temperature, yielding an N-doped porous nanocarbon. In this case, the addition of a second carbon source (e.g., FA) not only significantly promotes the graphitization of the resultant nanocarbon, but also aids in removing the metal species, thereby contributing to the fabrication of nanoporous structure while developing a metal-free electrocatalyst.

2.2. Multi-Doped Nanocarbon Electrocatalysts

Recently, double- or tertiary-doping of nitrogen, sulfur, and phosphorus into carbon has been further optimized for improvement toward the activity of the ORR [52]. Theoretical calculations have revealed that the S atom is positively charged and believed to be an effective catalytic center for ORR, whereas P-doping can enhance the charge delocalization of the carbon atoms and lead to carbon structures with increased edge sites. Recent pioneering work has indicated that the ORR performance of graphitic carbon may be further improved by co-doping heteroatoms, resulting in a synergistic effect arising from the charge and spin density changes, which are favorable toward O_2 adsorption, electron transfer, and facilitating the ORR performance [49]. This synergistic effect postulates that co-doped carbon materials may be able to achieve higher activity compared to their single atom doped counterparts [22,23,53,54]. By accurately tuning the organic linkers of MOFs component or through reasonable post-treatment methods, multi-doped nanocarbon (e.g., N, P, S-co-doped carbon) and related functional nanomaterials can be designed as ORR electrocatalysts [43–45]. For example, Dai and co-workers [46] reported the fabrication of N- and S-co-doped porous nanocarbon (N, S-MOFs-C) by using MOF-5 as the carbon precursor and template. Typically, urea and dimethyl sulfoxide (DMSO) are used respectively as nitrogen and sulfur precursors which were encapsulated into the pore structures of the MOF-5 template. Following a high temperature carbonization, the N, S-MOFs-C can be produced, demonstrating a high degree of graphitization, porous structure, and rich in number of N-Cx-, S-Cx-doping sites. In particular, X-ray photoelectron spectroscopy (XPS) analysis indicated that the treatment at 900 °C of MOF-5/organics resulted in an incorporation of 3.31 at % N and 1.08 at % S in the carbon lattice. The N, S-MOF-C (N: 3.31 at %, S: 1.08 at %) is used as an electrocatalyst to efficiently activate ORR in alkaline media, yielding comparable activity to state-of-the-art Pt/C catalysts. It was found that the ORR activity of N-doped nanocarbon catalyst is significantly increased with the addition of S-doping (based on the onset potential and current density at 0.6 V vs. RHE). Therefore, the spin and charge density of carbon atoms is an important factor in determining the number of active carbon atoms and results in the ORR activity of doped-nanocarbon. Thus, further understanding the crucial role of the doping microstructure on ORR performance is significant in the design and optimization of advanced metal-free carbon electrocatalysts.

2.3. MOF-Derived Nanocarbon Composite Electrocatalysts

Previous reports have demonstrated that incorporation of an ultrathin layer of MOF-derived nanocarbon on graphene oxide sheets could lead to the formation of a nanocarbon /graphene oxide/nanocarbon sandwich-like structure with high specific surface area and excellent electronic conductivity [28–31]. Initial efforts toward developing such a composite were conducted by Wang [29] and Zhang [31], via pyrolyzing ZIF-8/graphene oxide composite at a temperature of 800 °C. As shown in Figure 4, the resulting 2D sandwich-like nanocarbon/graphene/nanocarbon composite material demonstrated significantly enhanced ORR activity and stability. Owing to the presence of the graphene support, it was found that graphene-supported N-doped-nanocarbon (GNPC) provides close contact between the conductive graphene and N-doped nanocarbon. A sufficient balance between consecutive

electrical conductivity and number of active sites required for ORR is maintained by the thin layered N-doped nanocarbon. Thus the GNPC exhibits excellent electrocatalytic activity towards ORR, which is reflected by a high onset potential (0.92 V vs. RHE) as well as a high limiting current density (5.2 mA·cm^{-2} at 0.6 V) for oxygen reduction in alkaline media. Additionally, the GNPC also demonstrates long-term stability and enhanced methanol tolerance compared to Pt/C materials.

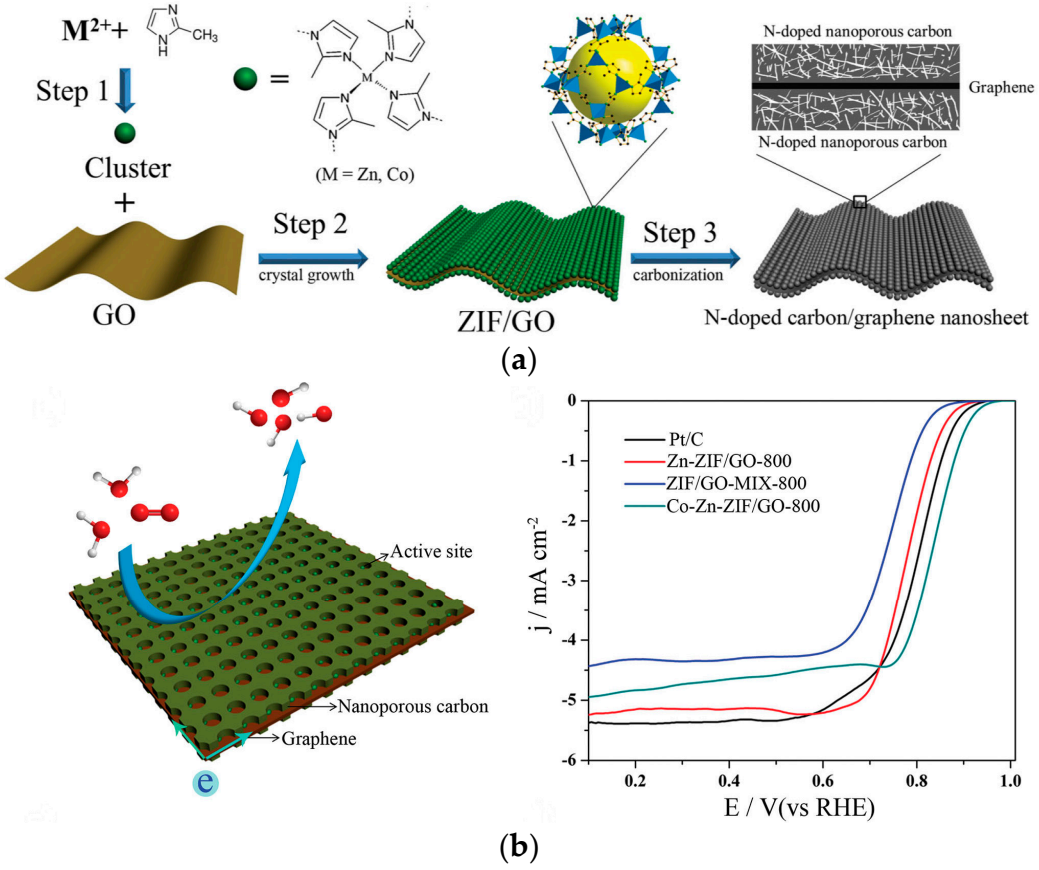

Figure 4. (**a**) The schematic synthesis of N-doped nanoporous carbon/graphene/ nanoporous carbon sandwiches; (**b**) Schematic oxygen reduction process conducted on the nanoporous carbon/graphene sheets in alkaline conditions; (**b**) LSV curves of commercial Pt/C, N-doped nanoporous carbon/graphene nanomaterials at 1600 rpm in O_2 saturated 0.1 M KOH solution [29]. Copyright 2015, WILEY-VCH Verlag GmbH & Co. KGaA, Weinheim.

In addition to the graphene support, carbon nanotubes (CNTs), and N-doped carbon nanotubes (NCNTs) used in the synthesis of nanocarbon composite materials have also demonstrated enhanced ORR activity and durability. Recently, N-doped graphitic porous nanocarbon (NGPC)/NCNTs composites as ORR catalysts operating in alkaline media have been investigated [21]. The well-known MOF-5 ([$Zn_4O(BDC)_3$], H_2BDC = benzene-1,4-dicarboxylate) combined with urea and nickel, have been employed as precursor and catalyst to develop a NGPC/NCNTs composite at 900 °C in N_2 atmosphere. As shown in Figure 5, the resulting NGPC/NCNTs catalyst contains NCNTs, ca. 30 nm in outer diameter and ca. 20 nm in joint length. The bamboo-like defects on the NCNTs are a typical morphological feature of N-doping and aids in providing active sites for O_2 adsorption. The ORR half-wave potential measured with the NGPC/NCNTs composite catalyst in 0.1 M KOH is by ca. 8 mV higher than that for Pt/C. Furthermore, a large cathodic current density (5.06 mA·cm^{-2}) was observed, with a value slightly higher than that found for Pt/C (4.76 mA·cm^{-2}). Notably, their work showed that the excellent ORR catalytic performance typically result from the unique heterostructure of NGPC/NCNTs composite. Based on the fact that the decrease of N-content in NGPC/NCNTs does

not lead to a proportional drop in ORR activity, the authors discovered that pyridinc-N and pyrrolic-N, located at graphitic plane sites, play a critical role for obtaining high ORR activity. Additionally, it was claimed that the degree of graphitization as well as high surface area of the NGPC/NCNTs catalyst exert great influence on the ORR activity.

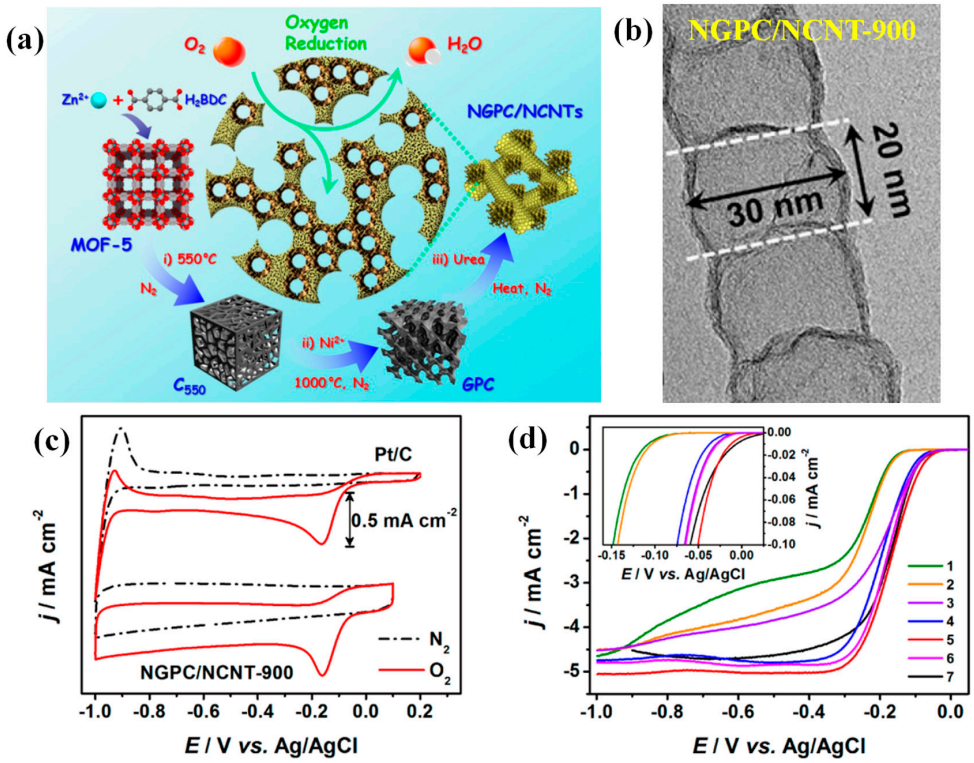

Figure 5. (**a**) Schematic illustration of the stepwise structural evolution from MOF-5 to NGPC/NCNTs; (**b**) HRTEM images of NCNTs in NGPC/NCNT-900; (**c**) Cyclic voltammograms of NGPC/NCNT-900 and Pt/C; (**d**) Linear-sweep voltammograms of GPC (trace 1), C-MOF-5 (trace 2), NPC (trace 3), NGPC/NCNT-800 (trace 4), NGPC/NCNT-900 (trace 5), NGPC/NCNT-1000 (trace 6), and Pt/C (trace 7) in O_2-saturated 0.1 M KOH with an electrode rotation speed of 1600 rpm [21]. Copyright 2015, American Chemical Society.

Besides Zn-based MOFs, Co-based MOFs (ZIF-67) have also been selected as a template and precursor to produce N-doped carbon nanotubes of hollow frameworks (NCNTFs) as an electrocatalyst [18]. The hollow frameworks constructed from interconnected crystalline NCNTs were synthesized by a simple thermal treatment of ZIF-67 in Ar/H_2 atmosphere. The morphology and structure of resultant NCNTF catalyst are shown in Figure 6. The SEM images demonstrate that NCNTFs with an interconnected NCNT-shell retain the polyhedron morphology of the initial ZIF-67. The advantages of choosing ZIF-67 as a precursor is the formation of highly uniform N-doping sites on the NCNTFs surface, as well as the incorporation of N-doped active sites into the graphitized nanocarbon alongside Co. It has been discovered that the advanced NCNTFs catalyst demonstrates improved ORR activity and stability compared to the Pt/C catalyst. The half-wave potential measured using NCNTFs catalyst in 0.1 M KOH is ca. 30 mV higher than that produced by Pt/C. It was worth mentioning that the ORR activity of the NCNTFs catalyst performs almost the best among the reported nanocarbon elelctrocatalysts derived from MOFs precursors. Table 1 gives a brief summary and comparison of the ORR activity of the MOF-derived nanocarbon electrocatalysts reported in recent literatures. More importantly, the developed NCNTFs catalyst demonstrates a bi-catalytic performance toward OER. The authors revealed that the exceptional electrocatalytic activity of the crystalline NCNTs ultimately comes down to their chemical composition and overall framework structure.

Pyrolysis temperature was also found to play a critical role toward the electrocatalytic activity of NCNTFs. The ORR activity of NCNTFs decreases as the pyrolysis temperature increased from 700 °C to 1000 °C, which reflected as a negative shift of the half-wave potential and decreased current density. This phenomenon may be related to the high density of defect sites generated on NCNTFs during the pyrolysis, which may favor O_2 adsorption. Since higher defective density can be produced at a lower pyrolysis temperature, NCNTFs-700 fabricated from the lower temperature exhibited the best ORR performance compared to its counterparts.

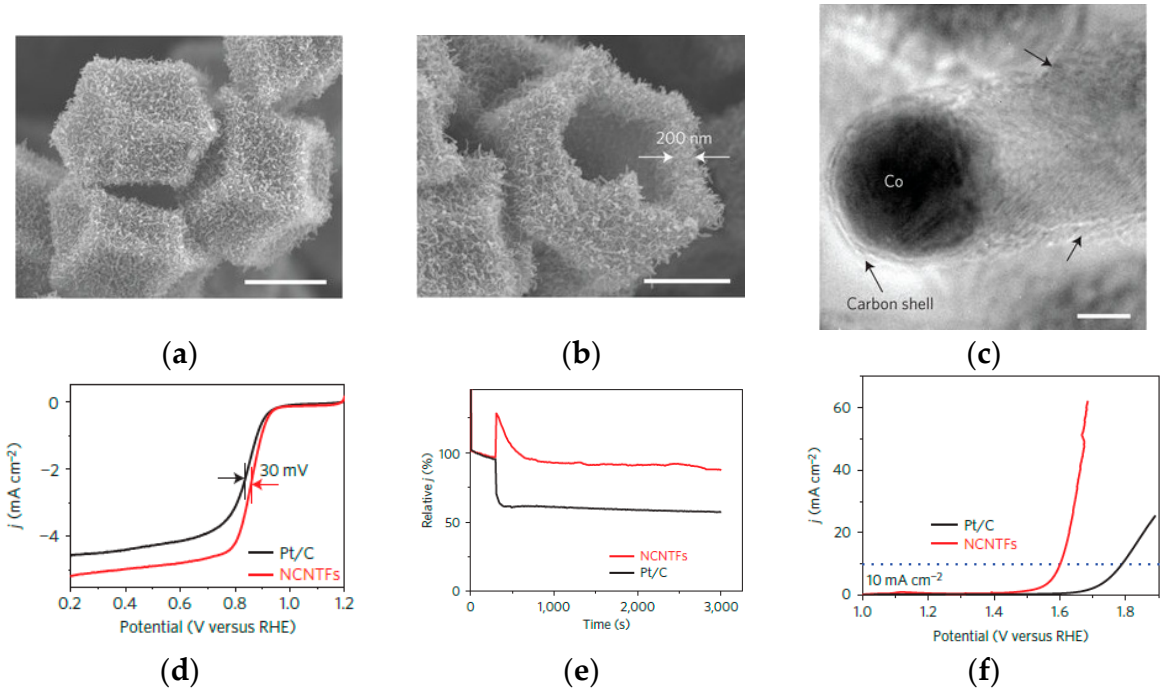

Figure 6. Morphology and structural characterization of NCNTFs obtained at 700 °C (**a**,**b**); FESEM images and (**c**) HRTEM images; (**d**) Electrochemical oxygen reduction on NCNTFs obtained at 700 °C; (**e**) Electrochemical methanol tolerance and durability of NCNTFs obtained at 700 °C; (**f**) Electrochemical oxygen evolution on NCNTFs obtained at 700 °C [18]. Copyright 2016, Nature Publishing Group.

Table 1. Summary of MOF-derived heteroatom-doped nanocarbon electrocatalysts with ORR activity reported in recent literatures.

MOF-Derived Nanocarbon Catalysts	Onset Potential	Limiting Current Density (mA·cm^{-2})	Electron Transfer Numbers	Ref.
ZIF-67 derived NCNTFs-700	0.97 V (vs. RHE)	-	3.97	[18]
NGPC/NCNT-900	−0.051 V (vs. Ag/AgCl)	5.06	4.0	[21]
P-N-Carbon-950	-	4.86	3.82	[24]
Zn-ZIF/GO-800	0.92 V (vs. RHE)	5.2	4.0	[29]
ZIF-8 derived NGPC	−0.02 V (vs. Ag/AgCl)	4.3	3.84	[37]

Table 1. *Cont.*

MOF-Derived Nanocarbon Catalysts	Onset Potential	Limiting Current Density ($mA \cdot cm^{-2}$)	Electron Transfer Numbers	Ref.
N, S-MOF-5-C	−0.005 V (vs. Ag/AgCl)	-	3.4–3.8	[46]
ZIF-derived carbon-L	0.86 V (vs. RHE)	4.6	3.68	[50]
MOF-5-CN900	0.035 V (vs. Hg/HgO)	4.2	3.12	[51]

3. MOF-Derived Transition Metal/Metal Oxide-Nanocarbon Electrocatalysts

Transition metal/ metal oxides, in particular cobalt/cobalt oxide and iron/iron oxide [26,32–36], are found to be active for oxygen reaction. However, inherent poor conductivity is one factor that limits the application of oxides as electrocatalysts in fuel cells. To solve this problem, coating these metal/metal oxide particles with the conductive nanocarbon for developing composite catalysts, has been considered as an effective strategy. Recently, a class of MOF-derived transition metal/metal oxide-nanocarbon composite catalysts have been extensively studied, particularly the cobalt/cobalt oxide-nanocarbon and iron/iron oxide-nanocarbon. The major advances of MOF-derived metal/nanocarbon composite catalysts is the synergistic effect occurring between the loaded transition metal nanoparticles and the nanocarbon matrix, resulting in significantly enhanced catalytic activity. Table 2 gives a brief summary of the transition metal/metal oxide-nanocarbon catalysts fabricated from MOFs with high ORR activity reported in recent literatures.

Table 2. Summary of MOF-derived metal/metal oxide-nanocarbon electrocatalysts with ORR activity reported in recent literatures.

MOF-Derived Catalysts	Onset Potential	Limiting Current Density ($mA \cdot cm^{-2}$)	Electron Transfer Numbers	Ref.
MIL-88B-Fe CNPs	1.03 V (vs. RHE)	8.31	3.97	[17]
ZIF-67-900	0.91 V (vs. RHE)	~5.0	-	[55]
P-CNCo-20	−0.04 V (vs. Ag/AgCl)	6.0	3.9	[56]
(Fe,Co)@GNC	0.91 V (vs. RHE)	-	3.7	[57]
$Co@Co_3O_4@C–CM$	0.93 V (vs. RHE)	-	3.8–3.9	[58]
$(r\text{-}GO\text{-}50\ wt\ \%\text{-}FeP)_n$-MOFs	−0.23 V (vs. Ag/AgCl)	6.2	4.0	[59]
$(Fe/Fe_3C@NGL\text{-}NCNT)$	0.04 V (vs. Ag/AgCl)	-	3.6	[60]
N-doped $Fe/Fe_3C@C/RGO$	1.0 V (vs. RHE)	10.12	3.08–3.52	[61]

3.1. MOF-Derived Cobalt/Cobalt Oxide-Nanocarbon Electrocatalysts

To date, carbon-supported Co/Co_3O_4 is one of the most extensively studied catalysts for oxygen reduction in fuel cells [58,62–64]. In 2014, Li and co-workers [55] proposed the application of Co-based MOFs (ZIF-67) as the precursor for fabricating the nanoporous Co-Nx-C hybrid, which can be used as an efficient ORR catalyst in both alkaline and acidic electrolyte. In their work, by optimizing

the pyrolysis temperature and acid leaching process, the developed Co-Nx-C hybrid catalyst with rich porosity and ordered graphitic structure exhibited outstanding ORR activity and good stability, suggesting that the ideal structure of highly dispersed Co-Nx active sites in the porous conductive nanocarbon system is essential to drive an ORR catalyst toward high performance. Moreover, it was also discovered that the ORR activity and stability increases as the size of the ZIF-67 precursor decreases from several micrometers to 300 nm. The Co-Nx-C hybrid prepared from the smallest size of ZIF-67 particles (ca. 300 nm) displayed the best performance toward the ORR, indicating that smaller particle size provides a larger surface area and facile access to catalytic centers, thus promoting enhanced mass and electron transfer. To develop rich and accessible active sites in Co-Nx-C composite catalyst, a series of bimetallic ZIFs (BMZIFs) grouping from ZIF-8 and ZIF-67, have been successfully synthesized in Jiang's group [56]. The BMZIFs-derived nanocarbon possesses both merits of carbon independently from ZIF-8 and ZIF-67, featuring a high degree of graphitization, large surface area, and highly dispersed C-Nx and Co-Nx-C active sites. As shown in Figure 7, among BMZIFs-derived nanocarbon, the product of CN-Co-20 (with Zn/Co molar ratio of 20) doped with N and Co as the best performer shows excellent ORR activity ($E_{onset} \approx -0.08$ V, and $E_{1/2} \approx -0.15$ V vs. Ag/AgCl) and even comparable to that of commercial Pt/C catalyst (20 wt % Pt, E-TEK). Remarkably, the authors discovered that extra doping CN-Co-20 catalyst with little amount of P atoms can further enhance the ORR performance. The P-doped-CNCo-20 nanocarbon presents dramatically more positive onset potential (−0.04 V vs. Ag/AgCl) and half-wave potential (−0.12 V vs. Ag/AgCl) as well as a higher diffusion-limited current density of 6.0 mA·cm^{-2} against its counterparts (e.g., CN-Co-20) and Pt/C. It was revealed that the superior ORR performance of P-CNCo-20 catalyst is derived from the high surface area and hierarchical porous nanostructure, uniform dispersion of P, N, Co dopants, as well as the synergistic effect arising from the nanocarbon and heteroatoms.

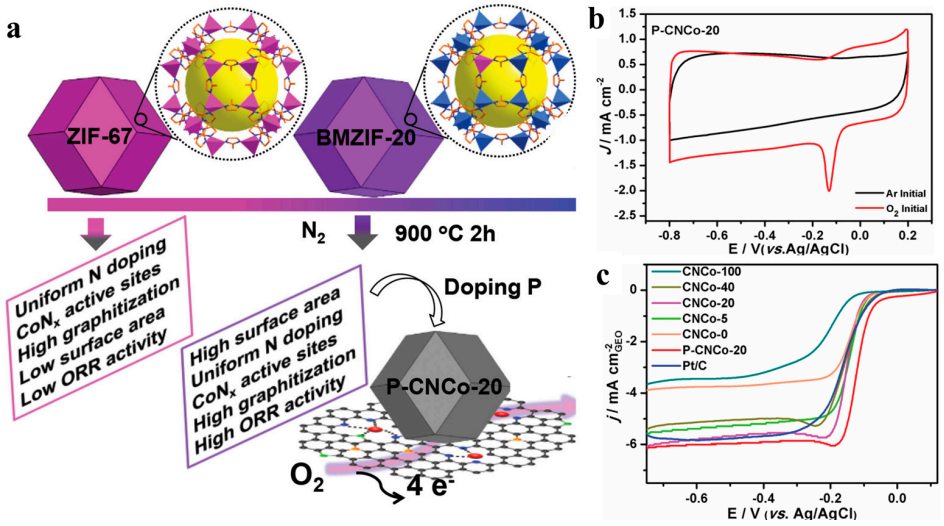

Figure 7. (**a**) Schematic illustration for the preparation of porous carbons from BMZIFs for highly efficient oxygen reduction reaction; (**b**) CV curves of P-CNCo-20 in Ar-saturated and O_2-saturated 0.1 M KOH; (**c**) LSV curves for different samples in O_2-saturated 0.1 M KOH at a rotation rate of 1600 rpm [56]. Copyright 2015, WILEY-VCH Verlag GmbH & Co. KGaA.

Additionally, Qiao and co-workers developed the MOF-derived hybrid of Co_3O_4/C porous nanowire arrays by using the precursor of Co-naphthalenedicarboxylate MOF-grown on Cu foil [62]. The inorganic and organic components in the MOFs structure were converted respectively into Co_3O_4 and nanocarbon via annealing under N_2 atmosphere, which resulted in the formation of hybrid nanowires with simultaneously generated pores inside. SEM and TEM images indicate that Co_3O_4/C nanowires have a smooth surface without any indication of morphologically dissimilar particles,

suggesting that all Co_3O_4 and C species are well integrated within the nanowire arrays (Figure 8). By combining the distinctive properties of Co_3O_4 with nanocarbon, and taking advantage of their uniform distribution, the obtained Co_3O_4/C-nanowire arrays exhibit enhanced catalytic performance compared to conventional electrode materials. As a bi-functional electrocatalyst, the hybrid Co_3O_4/C porous nanowire arrays can efficiently catalyze ORR and OER through a four-electron pathway, enabling reversible oxygen evolution and reduction. Notably, the excellent performance derives from the unique nanostructure. First, the in situ incorporation of nanocarbon into Co_3O_4/C nanowire arrays, assured by using MOFs as the precursor, leads to a structure with strongly interacting Co_3O_4 and nanocarbon matrix. Secondly, the conductive and porous structure is favorable to the rapid charge transfer and mass transport, which also ensures a smooth progression of the oxygen reaction.

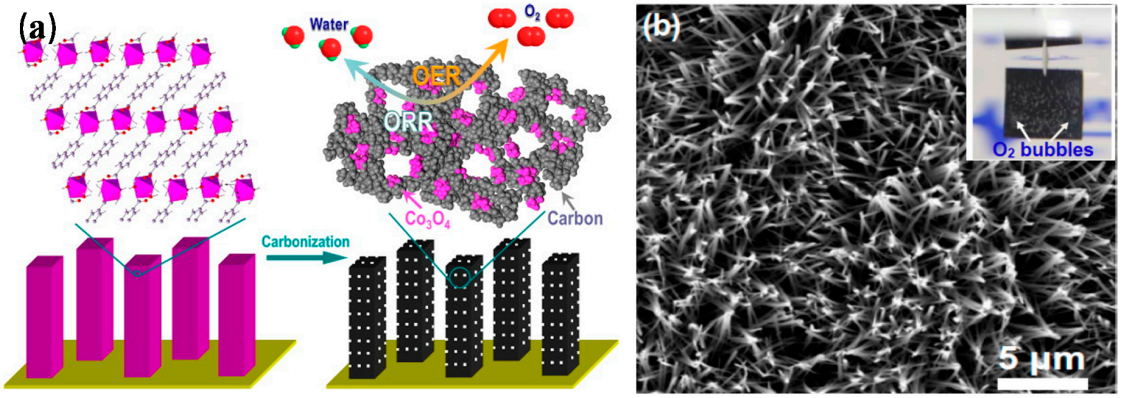

Figure 8. (**a**) Schematic illustration for the fabrication of Co_3O_4-carbon porous nanowire arrays; (**b**) SEM image of Co_3O_4-carbon porous nanowire arrays [62]. Copyright 2014, American Chemical Society.

Most of the MOF-derived catalytic materials are focused on either heteroatom-doped nanocarbon or in situ MOF-derived transition metal/metal oxide-carbon composites, which provide active sites for ORR catalysis but cannot maintain high activity [16,57,65]. Another drawback is the lack of enough effective space for diffusion of reactant (e.g., O_2, electrolyte) into active sites. To pursue advanced ORR catalysts, the properties of more exposed active sites and accessible surface area for rapid mass transport should be a research priority. Recently, Guo and co-workers demonstrated a new concept allowing ZIF-9 (synthesized from Co^{2+} and benzimidazole) to be used as a novel precursor for the in situ encapsulation of Co@Co_3O_4@C core@bishell nanoparticles into a highly ordered porous carbon matrix (CM) (denoted as Co@Co_3O_4@C–CM) [58]. The central cobalt ions in the ZIF-9-CM precursor are transformed into a fancy Co@Co_3O_4 core-shell nanostructure during a controlled oxidation process. The organic ligands (benzimidazole) from ZIF-9-CM are transformed into porous graphitic nanocarbon, which could wrap around the Co@Co_3O_4 nanocrystals, generating a novel Co@Co_3O_4@C core@bishell nanostructure. Meanwhile, through this synthesis method, a strong interaction between Co@Co_3O_4@C and CM support can be created. The most notable feature of the Co@Co_3O_4@C–CM structure is the adequate transport pathways that can facilitate the mass transport of O_2 and electrolyte. With the advances of interconnected porous channels, strong interactions between metal/oxide nanoparticles and carbon matrix, the unique Co@Co_3O_4@C–CM composite catalyst shows excellent activity toward ORR, reflected by the high positive onset potential of 0.93 V and a half-wave potential of 0.81 V (vs. RHE) in 0.1 M KOH solution. Moreover, it was found that the developed Co@Co_3O_4@C–CM composite catalyst also shows superior stability and better methanol tolerance compared to that of the commercial Pt/C catalyst.

3.2. MOF-Derived Iron/Iron Oxide-Nanocarbon Electrocatalysts

In addition to Co-based MOFs, other transition metal-based MOFs, like Fe-based MOFs, have also been reported as precursors in the fabrication of Fe-Nx-C and N-doped $Fe/Fe_3C@C/RGO$ catalysts to activate ORR in alkaline media [17,59–61,66]. Tang and co-workers [17] found that spindle-like Fe-based MOFs nanoparticles [MIL-88B-NH_3] can be synthesized using components of [$Fe_3O(H_2N\text{-}BDC)_3$] and 2-aminoterephtalic acid [H_2N-BDC]. With controllable size and shape (diameters of ~50 nm and lengths of ~140 nm), [MIL-88B-NH_3] features of well-defined porous structure and highly distributed Fe, N atoms. As both template and pyrolytic precursor, [MIL-88B-NH_3] can be employed to develop Fe-Nx-C nanostructure as an electrocatalyst (Figure 9). The developed Fe-Nx-C catalyst demonstrated enhanced ORR activity relative to Pt/C catalyst. The onset potential and half-wave potential of Fe-Nx-C catalyst for ORR was found to be 1.03 V and 0.92 V (vs. RHE) in 0.1 M KOH, respectively, representing the best ORR activity among non-noble metal catalysts. Deconvolution of N 1s XPS peaks discloses that the amino-N of the [MIL-88B-NH_3] precursor is completely changed into pyridine-N and quaternary-N after conversion into the Fe-Nx-C particles. Thus the most likely mechanism for the role of the Fe-Nx-C catalyst is that Fe may aid in catalyzing the graphitization process of the N/C precursor to form nanocarbon with more favorable N-doping sites for ORR. Also, Fe atoms are able to directly participate in Fe-Nx sites promising improved intrinsic activity. Additionally, the porosity structure derived from the MOFs particles could promote diffusion of both reactants (O_2) and products (OH^-), which promises the limiting current density of Fe-Nx-C catalyst is considerably 1.2 times higher than that of Pt/C.

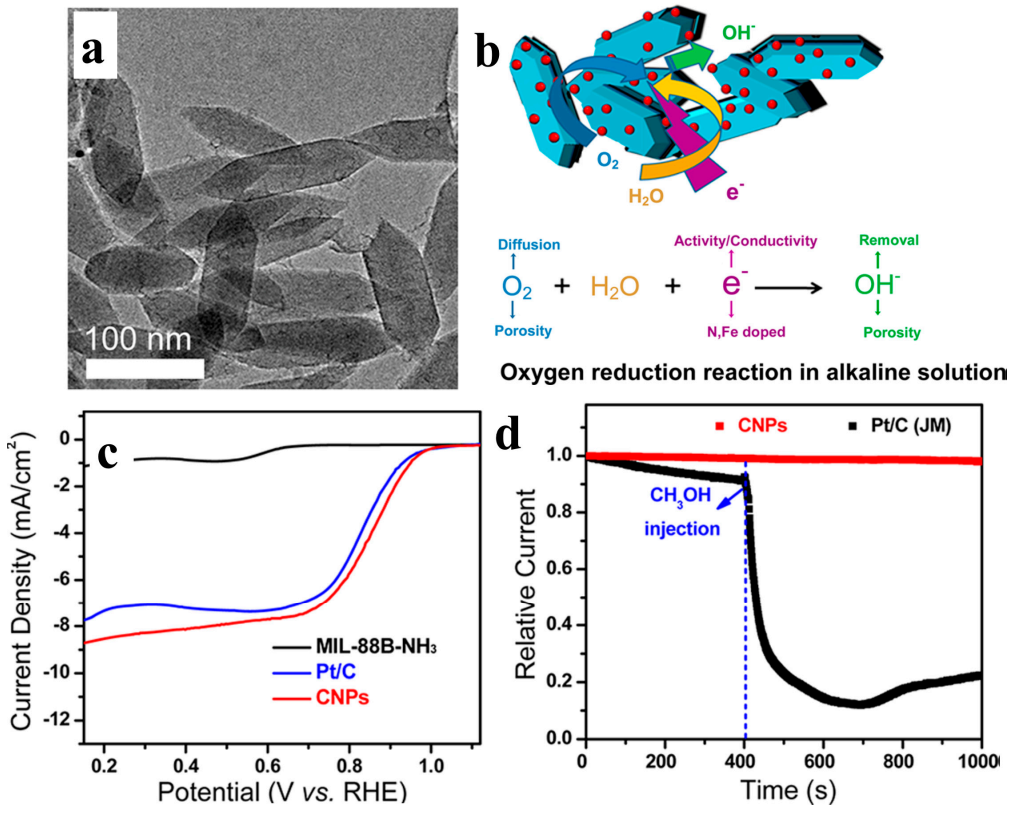

Figure 9. (**a**) TEM image of Fe/FeNx-C nanoparticles; (**b**) Illustration of high performance electrocatalysts for ORR in alkaline solution; (**c**) LSV curves of MIL-88B-NH_3, Fe/FeNx-C nanoparticles, and Pt/C at a rotation rate of 1600 rpm; (**d**) Chronoamperometric responses at 0.84 V in O_2-saturated 0.1 M KOH at Fe/FeNx-C (CNPs) or Pt/C electrodes (1600 rpm) before and after addition of 2 M methanol [17]. Copyright 2014, American Chemical Society.

Recently, nitrogen-doped reduced graphene oxide (NRGO) has been gaining interest as a candidate for catalyst support, due to its excellent electrical conductivity and high chemical stability [67]. It has been well documented that the fabrication of hybrid structure through collaboration of MOF-derived nanocarbon and NRGO might sufficiently exert their synergistic effect. In 2014, Chen and co-workers reported the fabrication of novel nitrogen-doped core-shell Fe/Fe_3C@C nanoboxes supported on graphene oxide (GO) sheets (N-doped Fe/Fe_3C@C/RGO) by a simple pyrolysis process, using GO as a conductive support and Prussian blue (PB-created from assembly of iron components with N-containing polyvinylpyrrolidone) nanocubes as carbon precursors [61]. During pyrolysis, the continuous decomposition of PB precursor was accompanied by the production of nitrogen-containing gases, resulting in the formation of a PB-nanocarbon with porous and N-doped structure. Since the N-containing species contributes to the reduction of GO, and N-doping in GO and PB-nanocarbon shells, the final product of N-doped core-shell-structured Fe/Fe_3C@C/RGO hybrid was evolved. As shown in Figure 10, the FESEM images suggest that the NRGO substrate also acts as a bridge to connect neighboring nanoboxes, thereby enhancing the overall electron transfer capability. Remarkably, the catalytic performance of the N-doped Fe/Fe_3C@C/RGO architecture displays much better ORR activity compared to N-doped Fe/Fe_3C@C without the RGO support. This excellent catalytic activity of N-doped Fe/Fe_3C@C/RGO is mainly generated by the synergistic effect of N-doped Fe/Fe_3C@C nanoboxes and NRGO sheets.

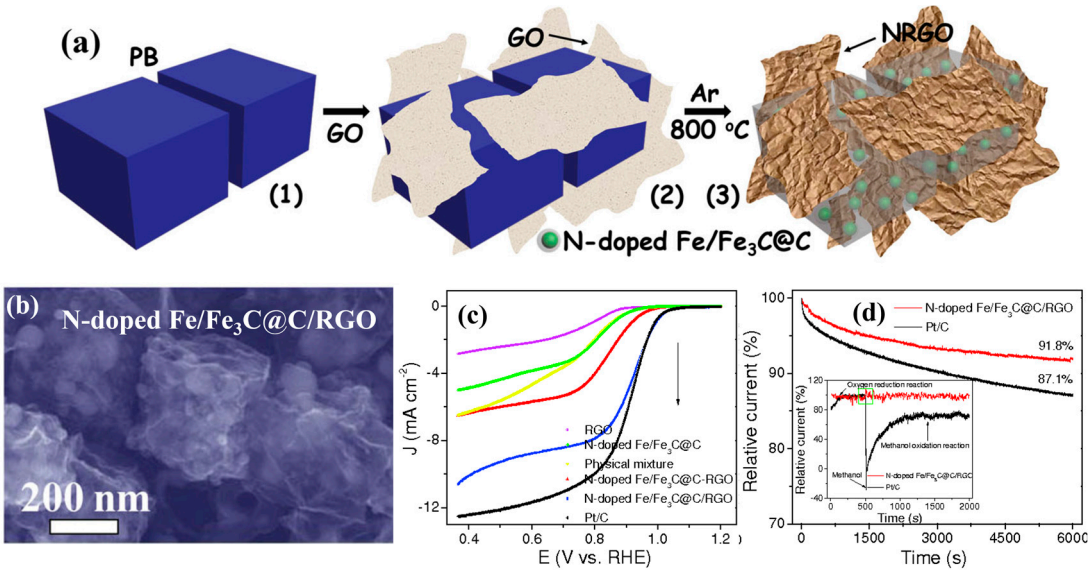

Figure 10. (**a**) Schematic illustration for the fabrication of N-doped Fe/Fe_3C@C/RGO; (**b**) FESEM images of N-doped Fe/Fe_3C@C/RGO; (**c**) LSV curves of RGO, N-doped Fe/Fe_3C@C, physical mixture-N-doped Fe/Fe_3C@C-RGO, N-doped Fe/Fe_3C@C/RGO, and Pt/C at a rotation rate of 1600 rpm in O_2-saturated 0.1 M KOH solution; (**d**) Current–time chronoamperometric response of N-doped Fe/Fe_3C@C/RGO and Pt/C at 0.8 V in O_2-saturated 0.1 M KOH solution (1600 rpm) [61]. Copyright 2014, WILEY-VCH Verlag GmbH & Co. KGaA.

3.3. Other MOF-Derived Metal-Nanocarbon Electrocatalysts

Besides several extensively investigated prototypical MOFs precursors, other kinds of metal-based-MOFs (e.g., Zr-MOFs, Cu-MOFs, Cd-MOFs, polyoxometalate-MOFs) [67–74] have also been explored as templates and/or precursors to prepare porous metal-nanocarbon electrocatalysts for fuel cells. Molybdenum dioxide (MoO_2) is an unusual transition metal oxide that has a high metallic-like electrical conductivity and superior durability, and has recently drawn great interest within the research community [75]. Both the Mo edge and O edge are active sites for the metal oxide and act as a key factor in promoting MoO_2 as an electrocatalyst. In 2015, Yu et al.

reported the fabrication of a porous molybdenum dioxide (MoO_2)/GO composite obtained from a polyoxometalate-based MOFs/graphene oxide (POMOFs/GO) precursor (as shown in Figure 11) [74]. Because the POMOFs precursor contains phosphorous (P), the final hybrid product was comprised of MoO_2, phosphorus-doped nanocarbon (PC), and RGO support (denoted as MoO_2@PC-RGO). In this POMOFs/GO-assisted strategy, a graphene sheet is a promising component to serve as a support material for electrocatalysts due to their unique 2D nanostructure, excellent electronic conductivity, and high electrochemical stability. Furthermore, the lone-pair electrons of the P atom located in the 3p orbital and vacant 3d orbital, can alter the charge state of the carbon surface and induce an alternate local charge density. Therefore, the combination of MoO_2 and P-doped nanocarbon can make contributions toward increasing the number of accessible active sites while simultaneously preventing the aggregation of MoO_2. The electrochemical results indicate that when GO (8.0 wt %) exists in MoO_2@PC-RGO, this composite catalyst exhibits dramatically enhanced hydrogen evolution reaction activity. In addition, a small amount of P doped in MoO_2@PC also provides a positive contribution to the hydrogen evolution activity.

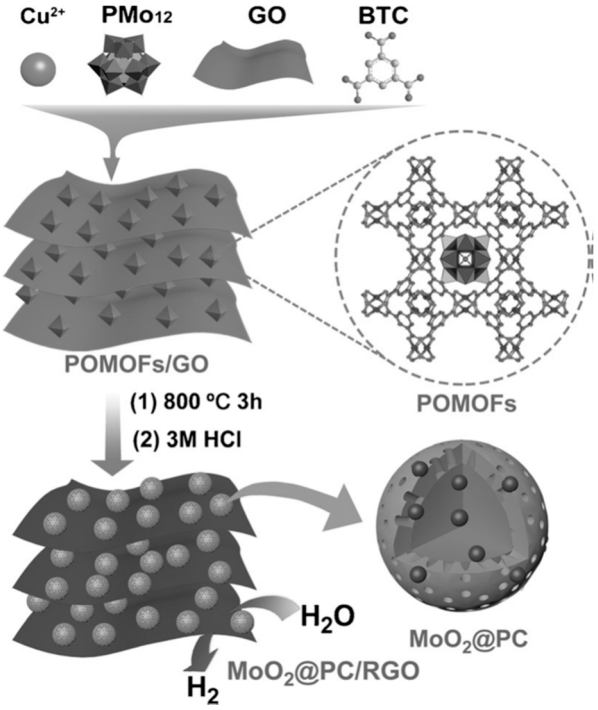

Figure 11. Illustration for the preparation of MoO_2@PC-RGO nanocomposite used as an electrocatalyst for the hydrogen evolution reaction (HER) [74]. Copyright 2015, WILEY-VCH Verlag GmbH & Co. KGaA.

4. Summary and Outlook

With a remarkable efficiency, high-energy density, and negligible emission of harmful gases, fuel cells are considered a green energy technology that meets the energy requirements to power future electrical vehicles and other energy-consuming devices. However, the high cost and poor durability of noble metal catalysts used in fuels cells limit their potential application within the consumer marketplace. Advanced electrode catalysts made from MOF template/precursor, with high activity and sufficient stability, as alternatives to noble metals are drawing considerable interest. Recent progresses toward MOF-derived nanocarbon catalysts, especially with the use of heteroatom-doped nanocarbon and transition metal-nanocarbon composites, have been summarized in this review. Firstly, Zn-based MOFs as precursor and template can be used to fabricate heteroatom-doped nanocarbon catalysts,

like N-doped nanocarbon, N, S-co-doped nanocarbon, as well as nanocarbon/CNTs, nanocarbon/GR composites. With rich active sites, highly accessible surface area, and ordered porous channels, these kinds of MOF-derived metal-free nanocarbon electrocatalysts demonstrate excellent ORR activity and long-term durability in alkaline media. While the heteroatom-doped nanocarbon with active doping sites is capable of building high activity for oxygen reduction, the presence of transition metal/metal oxide nanocrystal is essential to developing higher graphitized nanocarbon structures, yielding more conductive and even more active and durable catalysts. Additionally, the incorporation of transition metals within the doped-nanocarbon matrix, may aid in promoting the metal species to participate toward M-Nx-C sites, resulting in improved intrinsic activity.

Although MOF-derived nanocarbon catalysts are capable of efficiently catalyzing the ORR in alkaline media, they still suffer from low-activity and poor-durability in acidic environments. This observation indicates that most active sites for catalyzing ORR in both media are likely different due to alternate reaction mechanisms. Therefore, an understanding of how the rational design and synthesis during precursor development and subsequent post-treatment influences the generation and density of active sites is still necessary. Future efforts in the research and development of MOF-derived catalysts should focus on how to precisely control the interactions that occur between N-doped-nanocarbon and transition metal/metal oxide nanocrystals. Meanwhile, exploring alternative porous MOF precursors, using multi-transition metals, tuning precursor ratios, optimizing doping conditions, and modifying the support surface structure are anticipated to be possible strategies in further improving catalyst activity and performance durability.

Acknowledgments: This work was supported by the Natural Science and Engineering Research Council of Canada (NSERC), the Canada Research Chair Program (CRC), the Canada Foundation for Innovation (CFI), and the University of Western Ontario (UWO), Z. Song was supported by the Chinese Scholarship Council.

Conflicts of Interest: The authors declare no conflict of interest.

References

1. Debe, M.K. Electrocatalyst approaches and challenges for automotive fuel cells. *Nature* **2012**, *486*, 43–51. [CrossRef] [PubMed]
2. Cui, C.-H.; Yu, S.-H. Engineering interface and surface of noble metal nanoparticle nanotubes toward enhanced catalytic activity for fuel cell applications. *Acc. Chem. Res.* **2013**, *46*, 1427–1437. [CrossRef] [PubMed]
3. Zhang, Z.; Liu, J.; Gu, J.; Su, L.; Cheng, L. An overview of metal oxide materials as electrocatalysts and supports for polymer electrolyte fuel cells. *Energy Environ. Sci.* **2014**, *7*, 2535–2558. [CrossRef]
4. Zhong, C.-J.; Luo, J.; Njoki, P.N.; Mott, D.; Wanjala, B.; Loukrakpam, R.; Lim, S.; Wang, L.; Fang, B.; Xu, Z. Fuel cell technology: Nano-engineered multimetallic catalysts. *Energy Environ. Sci.* **2008**, *1*, 454–466. [CrossRef]
5. Cheng, N.; Banis, M.N.; Liu, J.; Riese, A.; Li, X.; Li, R.; Ye, S.; Knights, S.; Sun, X. Extremely stable platinum nanoparticles encapsulated in a zirconia nanocage by area-selective atomic layer deposition for the oxygen reduction reaction. *Adv. Mater.* **2015**, *27*, 277–281. [CrossRef] [PubMed]
6. Cheng, N.; Banis, M.N.; Liu, J.; Riese, A.; Mu, S.; Li, R.; Sham, T.-K.; Sun, X. Atomic scale enhancement of metal–support interactions between Pt and ZrC for highly stable electrocatalysts. *Energy Environ. Sci.* **2015**, *8*, 1450–1455. [CrossRef]
7. Rabis, A.; Rodriguez, P.; Schmidt, T.J. Electrocatalysis for polymer electrolyte fuel cells: Recent achievements and future challenges. *Acs Catal.* **2012**, *2*, 864–890. [CrossRef]
8. Cheng, N.; Mu, S.; Pan, M.; Edwards, P.P. Improved lifetime of PEM fuel cell catalysts through polymer stabilization. *Electrochem. Commun.* **2009**, *11*, 1610–1614. [CrossRef]
9. Jiang, Z.-Z.; Wang, Z.-B.; Chu, Y.-Y.; Gu, D.-M.; Yin, G.-P. Carbon riveted microcapsule Pt/MWCNTs-TiO_2 catalyst prepared by in situ carbonized glucose with ultrahigh stability for proton exchange membrane fuel cell. *Energy Environ. Sci.* **2011**, *4*, 2558–2566. [CrossRef]
10. Jung, N.; Chung, D.Y.; Ryu, J.; Yoo, S.J.; Sung, Y.-E. Pt-based nanoarchitecture and catalyst design for fuel cell applications. *Nano Today* **2014**, *9*, 433–456. [CrossRef]

11. Nie, Y.; Li, L.; Wei, Z. Recent advancements in Pt and Pt-free catalysts for oxygen reduction reaction. *Chem. Soc. Rev.* **2015**, *44*, 2168–2201. [CrossRef] [PubMed]
12. Wang, Y.-J.; Zhao, N.; Fang, B.; Li, H.; Bi, X.T.; Wang, H. Carbon-supported Pt-based alloy electrocatalysts for the oxygen reduction reaction in polymer electrolyte membrane fuel cells: Particle size, shape, and composition manipulation and their impact to activity. *Chem. Rev.* **2015**, *115*, 3433–3467. [CrossRef] [PubMed]
13. Morozan, A.; Jousselme, B.; Palacin, S. Low-platinum and platinum-free catalysts for the oxygen reduction reaction at fuel cell cathodes. *Energy Environ. Sci.* **2011**, *4*, 1238–1254. [CrossRef]
14. Jaouen, F.; Proietti, E.; Lefèvre, M.; Chenitz, R.; Dodelet, J.-P.; Wu, G.; Chung, H.T.; Johnston, C.M.; Zelenay, P. Recent advances in non-precious metal catalysis for oxygen-reduction reaction in polymer electrolyte fuel cells. *Energy Environ. Sci.* **2011**, *4*, 114–130. [CrossRef]
15. Zakaria, M.B.; Li, C.; Ji, Q.; Jiang, B.; Tominaka, S.; Ide, Y.; Hill, J.P.; Ariga, K.; Yamauchi, Y. Self-construction from 2D to 3D: One-pot layer-by-layer assembly of graphene oxide sheets held together by coordination polymers. *Angew. Chem.* **2016**, *55*, 8426–8430. [CrossRef] [PubMed]
16. Strickland, K.; Miner, E.; Jia, Q.; Tylus, U.; Ramaswamy, N.; Liang, W.; Sougrati, M.-T.; Jaouen, F.; Mukerjee, S. Highly active oxygen reduction non-platinum group metal electrocatalyst without direct metal-nitrogen coordination. *Nat. Commun.* **2015**, *6*, 7343. [CrossRef] [PubMed]
17. Zhao, S.; Yin, H.; Du, L.; He, L.; Zhao, K.; Chang, L.; Yin, G.; Zhao, H.; Liu, S.; Tang, Z. Carbonized nanoscale metal–organic frameworks as high performance electrocatalyst for oxygen reduction reaction. *ACS Nano* **2014**, *8*, 12660–12668. [CrossRef] [PubMed]
18. Xia, B.Y.; Yan, Y.; Li, N.; Wu, H.B.; Lou, X.W.D.; Wang, X. A metal–organic framework-derived bifunctional oxygen electrocatalyst. *Nat. Energy* **2016**, *1*, 15006. [CrossRef]
19. Zhao, S.; Liu, J.; Li, C.; Ji, W.; Yang, M.; Huang, H.; Liu, Y.; Kang, Z. Tunable ternary (N, P, B)-doped porous nanocarbons and their catalytic properties for oxygen reduction reaction. *ACS Appl. Mater. Interfaces* **2014**, *6*, 22297–22304. [CrossRef] [PubMed]
20. Geng, D.; Chen, Y.; Chen, Y.; Li, Y.; Li, R.; Sun, X.; Ye, S.; Knights, S. High oxygen-reduction activity and durability of nitrogen-doped graphene. *Energy Environ. Sci.* **2011**, *4*, 760–764. [CrossRef]
21. Zhang, L.; Wang, X.; Wang, R.; Hong, M. Structural evolution from metal–organic framework to hybrids of nitrogen-doped porous carbon and carbon nanotubes for enhanced oxygen reduction activity. *Chem. Mater.* **2015**, *27*, 7610–7618. [CrossRef]
22. Yang, W.; Yue, X.; Liu, X.; Zhai, J.; Jia, J. IL-derived N, S co-doped ordered mesoporous carbon for high-performance oxygen reduction. *Nanoscale* **2015**, *7*, 11956–11961. [CrossRef] [PubMed]
23. Gong, X.; Liu, S.; Ouyang, C.; Strasser, P.; Yang, R. Nitrogen-and phosphorus-doped biocarbon with enhanced electrocatalytic activity for oxygen reduction. *ACS Catal.* **2015**, *5*, 920–927. [CrossRef]
24. Fu, Y.; Huang, Y.; Xiang, Z.; Liu, G.; Cao, D. Phosphorous–nitrogen-codoped carbon materials derived from metal–organic frameworks as efficient electrocatalysts for oxygen reduction reactions. *Eur. J. Inorg. Chem.* **2016**, *2016*, 2100–2105. [CrossRef]
25. Zhao, Y.; Song, Z.; Li, X.; Sun, Q.; Cheng, N.; Lawes, S.; Sun, X. Metal organic frameworks for energy storage and conversion. *Energy Storage Mater.* **2016**, *2*, 35–62. [CrossRef]
26. Xia, W.; Mahmood, A.; Zou, R.; Xu, Q. Metal–organic frameworks and their derived nanostructures for electrochemical energy storage and conversion. *Energy Environ. Sci.* **2015**, *8*, 1837–1866. [CrossRef]
27. Fujita, M.; Kwon, Y.J.; Washizu, S.; Ogura, K. Preparation, clathration ability, and catalysis of a two-dimensional square network material composed of cadmium (II) and 4, 4′-bipyridine. *J. Am. Chem. Soc.* **1994**, *116*, 1151–1152. [CrossRef]
28. Jiao, L.; Zhou, Y.-X.; Jiang, H.-L. Metal–organic framework-based CoP/reduced graphene oxide: High-performance bifunctional electrocatalyst for overall water splitting. *Chem. Sci.* **2016**, *7*, 1690–1695. [CrossRef]
29. Wei, J.; Hu, Y.; Liang, Y.; Kong, B.; Zhang, J.; Song, J.; Bao, Q.; Simon, G.P.; Jiang, S.P.; Wang, H. Nitrogen-Doped Nanoporous Carbon/Graphene Nano-Sandwiches: Synthesis and Application for Efficient Oxygen Reduction. *Adv. Funct. Mater.* **2015**, *25*, 5768–5777. [CrossRef]
30. Ge, L.; Yang, Y.; Wang, L.; Zhou, W.; De Marco, R.; Chen, Z.; Zou, J.; Zhu, Z. High activity electrocatalysts from metal–organic framework-carbon nanotube templates for the oxygen reduction reaction. *Carbon* **2015**, *82*, 417–424. [CrossRef]

31. Zhong, H.-X.; Wang, J.; Zhang, Y.-W.; Xu, W.-L.; Xing, W.; Xu, D.; Zhang, Y.-F.; Zhang, X.-B. ZIF-8 derived graphene-based nitrogen-doped porous carbon sheets as highly efficient and durable oxygen reduction electrocatalysts. *Angew. Chem. Int. Ed.* **2014**, *53*, 14235–14239. [CrossRef] [PubMed]
32. Santos, V.P.; Wezendonk, T.A.; Jaén, J.J.D.; Dugulan, A.I.; Nasalevich, M.A.; Islam, H.-U.; Chojecki, A.; Sartipi, S.; Sun, X.; Hakeem, A.A. Metal organic framework-mediated synthesis of highly active and stable Fischer-Tropsch catalysts. *Nat. Commun.* **2015**, *6*, 6451. [CrossRef] [PubMed]
33. Das, R.; Pachfule, P.; Banerjee, R.; Poddar, P. Metal and metal oxide nanoparticle synthesis from metal organic frameworks (MOFs): Finding the border of metal and metal oxides. *Nanoscale* **2012**, *4*, 591–599. [CrossRef] [PubMed]
34. Zhang, L.; Wu, H.B.; Madhavi, S.; Hng, H.H.; Lou, X.W. Formation of Fe_2O_3 microboxes with hierarchical shell structures from metal–organic frameworks and their lithium storage properties. *J. Am. Chem. Soc.* **2012**, *134*, 17388–17391. [CrossRef] [PubMed]
35. Zhao, J.; Wang, F.; Su, P.; Li, M.; Chen, J.; Yang, Q.; Li, C. Spinel $ZnMn_2O_4$ nanoplate assemblies fabricated via "escape-by-crafty-scheme" strategy. *J. Mater. Chem.* **2012**, *22*, 13328–13333. [CrossRef]
36. Hu, L.; Huang, Y.; Zhang, F.; Chen, Q. CuO/Cu_2O composite hollow polyhedrons fabricated from metal–organic framework templates for lithium-ion battery anodes with a long cycling life. *Nanoscale* **2013**, *5*, 4186–4190. [CrossRef] [PubMed]
37. Zhang, L.; Su, Z.; Jiang, F.; Yang, L.; Qian, J.; Zhou, Y.; Li, W.; Hong, M. Highly graphitized nitrogen-doped porous carbon nanopolyhedra derived from ZIF-8 nanocrystals as efficient electrocatalysts for oxygen reduction reactions. *Nanoscale* **2014**, *6*, 6590–6602. [CrossRef] [PubMed]
38. Chaikittisilp, W.; Ariga, K.; Yamauchi, Y. A new family of carbon materials: Synthesis of MOF-derived nanoporous carbons and their promising applications. *J. Mater. Chem. A* **2013**, *1*, 14–19. [CrossRef]
39. Liu, B.; Shioyama, H.; Akita, T.; Xu, Q. Metal-organic framework as a template for porous carbon synthesis. *J. Am. Chem. Soc.* **2008**, *130*, 5390–5391. [CrossRef] [PubMed]
40. Zhu, C.; Li, H.; Fu, S.; Du, D.; Lin, Y. Highly efficient nonprecious metal catalysts towards oxygen reduction reaction based on three-dimensional porous carbon nanostructures. *Chem. Soc. Rev.* **2016**, *45*, 517–531. [CrossRef] [PubMed]
41. Dai, L.; Xue, Y.; Qu, L.; Choi, H.-J.; Baek, J.-B. Metal-free catalysts for oxygen reduction reaction. *Chem. Rev.* **2015**, *115*, 4823–4892. [CrossRef] [PubMed]
42. Su, D.S.; Perathoner, S.; Centi, G. Nanocarbons for the development of advanced catalysts. *Chem. Rev.* **2013**, *113*, 5782–5816. [CrossRef] [PubMed]
43. Liu, Z.-W.; Peng, F.; Wang, H.-J.; Yu, H.; Zheng, W.-X.; Yang, J. Phosphorus-doped graphite layers with high electrocatalytic activity for the O_2 reduction in an alkaline medium. *Angew. Chem. Int. Ed.* **2011**, *50*, 3257–3261. [CrossRef] [PubMed]
44. Li, H.; Liu, H.; Jong, Z.; Qu, W.; Geng, D.; Sun, X.; Wang, H. Nitrogen-doped carbon nanotubes with high activity for oxygen reduction in alkaline media. *Int. J. Hydrog. Energy* **2011**, *36*, 2258–2265. [CrossRef]
45. Wang, X.; Liu, R.; Waje, M.M.; Chen, Z.; Yan, Y.; Bozhilov, K.N.; Feng, P. Sulfonated ordered mesoporous carbon as a stable and highly active protonic acid catalyst. *Chem. Mater.* **2007**, *19*, 2395–2397. [CrossRef]
46. Li, J.; Chen, Y.; Tang, Y.; Li, S.; Dong, H.; Li, K.; Han, M.; Lan, Y.-Q.; Bao, J.; Dai, Z. Metal-organic framework templated nitrogen and sulfur co-doped porous carbons as highly efficient metal-free electrocatalysts for oxygen reduction reactions. *J. Mater. Chem. A* **2014**, *2*, 6316–6319. [CrossRef]
47. Gong, K.; Du, F.; Xia, Z.; Durstock, M.; Dai, L. Nitrogen-doped carbon nanotube arrays with high electrocatalytic activity for oxygen reduction. *Science* **2009**, *323*, 760–764. [CrossRef] [PubMed]
48. Liu, R.; Wu, D.; Feng, X.; Müllen, K. Nitrogen-doped ordered mesoporous graphitic arrays with high electrocatalytic activity for oxygen reduction. *Angew. Chem.* **2010**, *122*, 2619–2623. [CrossRef]
49. Yang, W.; Fellinger, T.; Antonietti, M. Efficient metal-free oxygen reduction in alkaline medium on high-surface-area mesoporous nitrogen-doped carbons made from ionic liquids and nucleobases. *J. Am. Chem. Soc.* **2010**, *133*, 206–209. [CrossRef] [PubMed]
50. Zhang, P.; Sun, F.; Xiang, Z.; Shen, Z.; Yun, J.; Cao, D. ZIF-derived in situ nitrogen-doped porous carbons as efficient metal-free electrocatalysts for oxygen reduction reaction. *Energy Environ. Sci.* **2014**, *7*, 442–450. [CrossRef]

51. Pandiaraj, S.; Aiyappa, H.B.; Banerjee, R.; Kurungot, S. Post modification of MOF derived carbon via g-C_3N_4 entrapment for an efficient metal-free oxygen reduction reaction. *Chem. Commun.* **2014**, *50*, 3363–3366. [CrossRef] [PubMed]
52. Choi, C.H.; Park, S.H.; Woo, S.I. Binary and ternary doping of nitrogen, boron, and phosphorus into carbon for enhancing electrochemical oxygen reduction activity. *ACS Nano* **2012**, *6*, 7084–7091. [CrossRef] [PubMed]
53. Ranjbar Sahraie, N.; Paraknowitsch, J.P.; Gobel, C.; Thomas, A.; Strasser, P. Noble-metal-free electrocatalysts with enhanced ORR performance by task-specific functionalization of carbon using ionic liquid precursor systems. *J. Am. Chem. Soc.* **2014**, *136*, 14486–14497. [CrossRef] [PubMed]
54. Zhang, M.; Dai, L. Carbon nanomaterials as metal-free catalysts in next generation fuel cells. *Nano Energy* **2012**, *1*, 514–517. [CrossRef]
55. Wang, X.; Zhou, J.; Fu, H.; Li, W.; Fan, X.; Xin, G.; Zheng, J.; Li, X. MOF derived catalysts for electrochemical oxygen reduction. *J. Mater. Chem. A* **2014**, *2*, 14064–14070. [CrossRef]
56. Chen, Y.Z.; Wang, C.; Wu, Z.Y.; Xiong, Y.; Xu, Q.; Yu, S.H.; Jiang, H.L. From Bimetallic Metal-Organic Framework to Porous Carbon: High Surface Area and Multicomponent Active Dopants for Excellent Electrocatalysis. *Adv. Mater.* **2015**, *27*, 5010–5016. [CrossRef] [PubMed]
57. Xi, J.; Xia, Y.; Xu, Y.; Xiao, J.; Wang, S. (Fe, Co)@ nitrogen-doped graphitic carbon nanocubes derived from polydopamine-encapsulated metal–organic frameworks as a highly stable and selective non-precious oxygen reduction electrocatalyst. *Chem. Commun.* **2015**, *51*, 10479–10482. [CrossRef] [PubMed]
58. Xia, W.; Zou, R.; An, L.; Xia, D.; Guo, S. A metal-organic framework route to in situ encapsulation of Co@Co_3O_4@C core@bishell nanoparticles into a highly ordered porous carbon matrix for oxygen reduction. *Energy Environ. Sci.* **2015**, *8*, 568–576. [CrossRef]
59. Proietti, E.; Jaouen, F.; Lefèvre, M.; Larouche, N.; Tian, J.; Herranz, J.; Dodelet, J.-P. Iron-based cathode catalyst with enhanced power density in polymer electrolyte membrane fuel cells. *Nat. Commun.* **2011**, *2*, 416. [CrossRef] [PubMed]
60. Li, J.-S.; Li, S.-L.; Tang, Y.-J.; Han, M.; Dai, Z.-H.; Bao, J.-C.; Lan, Y.-Q. Nitrogen-doped Fe/Fe_3C@graphitic layer/carbon nanotube hybrids derived from MOFs: Efficient bifunctional electrocatalysts for ORR and OER. *Chem. Commun.* **2015**, *51*, 2710–2713. [CrossRef] [PubMed]
61. Hou, Y.; Huang, T.; Wen, Z.; Mao, S.; Cui, S.; Chen, J. Metal-Organic Framework-Derived Nitrogen-Doped Core-Shell-Structured Porous Fe/Fe_3C@ C Nanoboxes Supported on Graphene Sheets for Efficient Oxygen Reduction Reactions. *Adv. Energy Mater.* **2014**, *4*, 1400337. [CrossRef]
62. Li, X.; Fang, Y.; Lin, X.; Tian, M.; An, X.; Fu, Y.; Li, R.; Jin, J.; Ma, J. Metal–organic framework derived hybrid Co_3O_4-carbon porous nanowire arrays as reversible oxygen evolution electrodes. *J. Am. Chem. Soc.* **2014**, *136*, 13925–13931.
63. Xia, W.; Zou, R.; An, L.; Xia, D.; Guo, S. MOF derived Co_3O_4 nanoparticles embedded in N-doped mesoporous carbon layer/MWCNT hybrids: Extraordinary bi-functional electrocatalysts for OER and ORR. *J. Mater. Chem. A* **2015**, *3*, 17392–17402.
64. Chaikittisilp, W.; Torad, N.L.; Li, C.; Imura, M.; Suzuki, N.; Ishihara, S.; Ariga, K.; Yamauchi, Y. Synthesis of Nanoporous Carbon–Cobalt-Oxide Hybrid Electrocatalysts by Thermal Conversion of Metal–Organic Frameworks. *Chem. A Eur. J.* **2014**, *20*, 4217–4221. [CrossRef] [PubMed]
65. Banham, D.; Ye, S.; Pei, K.; Ozaki, J.-i.; Kishimoto, T.; Imashiro, Y. A review of the stability and durability of non-precious metal catalysts for the oxygen reduction reaction in proton exchange membrane fuel cells. *J. Power Sources* **2015**, *285*, 334–348. [CrossRef]
66. Jahan, M.; Bao, Q.; Loh, K.P. Electrocatalytically Active Graphene–Porphyrin MOF Composite for Oxygen Reduction Reaction. *J. Am. Chem. Soc.* **2012**, *134*, 6707–6713. [CrossRef] [PubMed]
67. Jahan, M.; Liu, Z.; Loh, K.P. A Graphene Oxide and Copper-Centered Metal Organic Framework Composite as a Tri-Functional Catalyst for HER, OER, and ORR. *Adv. Funct. Mater.* **2013**, *23*, 5363–5372. [CrossRef]
68. Lin, Q.; Bu, X.; Kong, A.; Mao, C.; Zhao, X.; Bu, F.; Feng, P. New Heterometallic Zirconium Metalloporphyrin Frameworks and Their Heteroatom-Activated High-Surface-Area Carbon Derivatives. *J. Am. Chem. Soc.* **2015**, *137*, 2235–2238. [CrossRef] [PubMed]
69. Zhao, C.-W.; Li, Y.-A.; Wang, X.-R.; Chen, G.-J.; Liu, Q.-K.; Ma, J.-P.; Dong, Y.-B. Fabrication of Cd (ii)-MOF-based ternary photocatalytic composite materials for H 2 production via a gel-to-crystal approach. *Chem. Commun.* **2015**, *51*, 15906–15909. [CrossRef] [PubMed]

70. Chen, C.; Kang, Y.; Huo, Z.; Zhu, Z.; Huang, W.; Xin, H.L.; Snyder, J.D.; Li, D.; Herron, J.A.; Mavrikakis, M. Highly crystalline multimetallic nanoframes with three-dimensional electrocatalytic surfaces. *Science* **2014**, *343*, 1339–1343. [CrossRef] [PubMed]
71. Li, Z.; Yu, R.; Huang, J.; Shi, Y.; Zhang, D.; Zhong, X.; Wang, D.; Wu, Y.; Li, Y. Platinum-nickel frame within metal-organic framework fabricated in situ for hydrogen enrichment and molecular sieving. *Nat. Commun.* **2015**, *6*, 8248. [CrossRef] [PubMed]
72. Mao, J.; Yang, L.; Yu, P.; Wei, X.; Mao, L. Electrocatalytic four-electron reduction of oxygen with Copper (II)-based metal-organic frameworks. *Electrochem. Commun.* **2012**, *19*, 29–31. [CrossRef]
73. Li, J.-S.; Tang, Y.-J.; Liu, C.-H.; Li, S.-L.; Li, R.-H.; Dong, L.-Z.; Dai, Z.-H.; Bao, J.-C.; Lan, Y.-Q. Polyoxometalate-based metal-organic framework-derived hybrid electrocatalysts for highly efficient hydrogen evolution reaction. *J. Mater. Chem. A* **2016**, *4*, 1202–1207. [CrossRef]
74. Tang, Y.J.; Gao, M.R.; Liu, C.H.; Li, S.L.; Jiang, H.L.; Lan, Y.Q.; Han, M.; Yu, S.H. Porous Molybdenum-Based Hybrid Catalysts for Highly Efficient Hydrogen Evolution. *Angew. Chem. Int. Ed.* **2015**, *54*, 12928–12932. [CrossRef] [PubMed]
75. Katrib, A.; Leflaive, P.; Hilaire, L.; Maire, G. Molybdenum based catalysts. I. MoO_2 as the active species in the reforming of hydrocarbons. *Catal. Lett.* **1996**, *38*, 95–99. [CrossRef]